



# Effect of Oxygen Doping on the Synthesis of Green Cadmium Sulfide for Ciprofloxacin Photocatalytic Degradation

**Gunawan<sup>\*1</sup>, Didik Setiyo Widodo<sup>1</sup>, Akbar Setyawan<sup>1</sup>, Mariana Sada Bii<sup>1</sup>, Roni Adi Wijaya<sup>1</sup>**

<sup>1</sup>Chemistry Department, Diponegoro University, Semarang 50275 Indonesia

## Abstract

This study describes the synthesis of cadmium sulfide (CdS) modified through green synthesis and doped with oxygen (CdS-O), followed by testing its effectiveness in ciprofloxacin photocatalytic degradation. Green synthesis using tea powder produces smaller CdS particles. Green synthesis using tea powder resulted in smaller particles and oxygen doping, helping to reduce the band gap and increasing its effectiveness in the photodegradation of ciprofloxacin. The synthesized CdS and CdS-O characterized using FTIR, XRD, SEM-EDS, and UV-DRS. FTIR and XRD characterization confirmed the formation of CdS. SEM analysis revealed that CdS particles have a smooth, spherical surface, while CdS-O particles exhibit a coral-like structure. Oxygen doping reduced the band gap of CdS from 2.37 eV to 2.35 eV. The Ciprofloxacin (CIP) degradation results showed that CdS-O achieved a better degradation effect than CdS, with a degradation percentage reaching 58.5%. This highlights the development potential of CdS green synthesis methods and modified enhanced photocatalytic properties for wastewater treatment.

**Keywords:** Photocatalyst, green synthesis, cadmium sulfide, ciprofloxacin

**Full-length article** \*Corresponding Author, e-mail: [gunawan@live.undip.ac.id](mailto:gunawan@live.undip.ac.id)

Doi # <https://doi.org/10.62877/67-IJCBS-24-25-19-67>

## 1. Introduction

Photocatalysis is a treatment technique for water remediation that attracts wide interest due to its environmentally friendly methods and operation [1]. This method has good potential to address water pollution caused by harmful organic compounds such as antibiotics [2]. Ciprofloxacin, a widely used antibiotic, frequently detected in wastewater and aquatic environments, posing risks to ecosystems and human health. Ciprofloxacin is an antibiotic fluoroquinolone class that is most commonly used. This antibiotic creates waste that can affect environmental conditions, such as creating conditions where many bacteria become resistant to antibiotics [3-4]. Photo catalyst activity comes from a hydroxyl radical resulting from electron hole pairs ( $e^-/h^+$ ) generated when photon energy exceeds the band gap value. Electrons ( $e^-$ ) then settle in the conduction band (CB) after leaving their place in the valence band (VB), producing holes ( $h^+$ ) in the valence band [5-6].

The photo catalysis activity depends on semiconductor characteristics, where the properties of photo catalysts modified through techniques and methods used for synthesis to control particle size and shape [7]. Cadmium sulfide (CdS) is a semiconductor compound with a band gap of 2.4 eV. It is suitable for photo catalytic activity because it features visible light absorption [8]. CdS efficiently absorbs visible light at wavelengths up to 530 nm. The photo catalytic

activity of CdS affected by the synthesis conditions and methods, its structure, morphology, particle size, surface area, and crystallinity [9]. Several CdS synthesis methods developed, including hydrothermal, co-precipitation, sol-gel, and green synthesis [10-11]. The green synthesis method has recently attracted attention because of its environmentally friendly process and ability to produce particles with smaller sizes and more even distribution. CdS powder obtained by green synthesis from plant-based materials containing several substances, such as flavonoids, catechins, and epigallocatechin gallate (EGCG), which play an important role in nanoparticle formation [12]. Research by Tudu et al. [13] successfully obtained CdS as nanoparticles from mushrooms. Munyai et al. [14] extracted the leaves of *Sutherlandia frutescens* (*S. frutescens*) and produced cadmium Sulfide (CdS) nanostructures, which are effective in photodegrading Malachite green dye. In addition, modification efforts to improve the effectiveness are also required to overcome the relatively large band gap and high recombination rate of electron-hole pairs. Various modification methods, such as doping with certain elements, carried out to improve the photocatalytic performance of CdS. Research by et al. Esra et al. [15] using Ag doping can increase its photocatalytic activity, and Zein et al. [16] used Fe as doping to doping to improve the optical properties of CdS. On the other hand, developments in doping oxygen in

semiconductors reported to reduce the band gap and increase charge separation, help form more semiconductor charge carriers, increase car semiconductors, and improve carrier mobility and material stability [17-21]. Therefore, this study aims to synthesize CdS using the green method using tea powder and doping it with oxygen (CdS-O) to improve the photocatalytic performance in the photodegradation of ciprofloxacin. Characterization performed using FTIR, XRD, SEM-EDS, and UV-DRS to analyze the structure, morphology, and optical properties of the materials produced. The results of this study expected to provide new insights into developing more efficient and environmentally friendly photo catalysts for wastewater treatment applications.

## 2. Materials and methods

Materials used were cadmium sulfate hydrate ( $3\text{CdSO}_4 \cdot 8\text{H}_2\text{O}$ ) (Merck), natrium sulfide ( $\text{Na}_2\text{S}$ ) (Merck), Methanol ( $\text{CH}_3\text{OH}$ ) (Merck), tea bag powder (trade), oxygen (Pure Air), ciprofloxacin 98% (Sigma), deionized water, distilled water. The tools used were glassware (Herma), filter paper (Whatman no.42), a 1 mL volume pipette (Sigma), 1 mL volume pipette (Iwaki), visible light (Ivaco IP 66, 200 W), analytical balance (Ohaus, Model PA323), furnace (Nabertherm), Tubular Furnace (handmade), centrifuge (Hettich Zentrifugen), photo catalytic reactor (handmade). UV-Vis spectrophotometer (Genesys 10S), FTIR spectrophotometer (PerkinElmer Frontier, Integrated Laboratory, UNDIP), SEM-EDX (Phenom Desktop ProXL, Swift ED3000, Integrated Laboratory, UII), XRD (Bruker D2 Phaser, Integrated Laboratory, UII), UV-DRS spectrophotometer (Shimadzu U-2450, Laboratory, UI) were used for characterization analysis.

### 2.1. Solution Preparation

The solution was made by mixing 3.848 grams of  $3\text{CdSO}_4 \cdot 8\text{H}_2\text{O}$  and 0.39 grams of  $\text{Na}_2\text{S}$ . Then, each was dissolved in a 10 mL volumetric flask using distilled water to obtain a solution of 0.5 M  $\text{CdSO}_4$  and 0.5 M  $\text{Na}_2\text{S}$ .

### 2.2. Green Synthesis of Cadmium Sulfide

0.5 grams of tea powder was mixed in 30 mL of methanol and left in a dark room for 1 day. After 1 day, filtering was done to separate the tea sediment from the solution. The extract was added to 2 mL of 0.5 M  $\text{CdSO}_4$  solution and left in the dark for 3 days, followed by adding 0.5 mL of 0.5 M  $\text{Na}_2\text{S}$  solution and left in the dark for 4 days. The precipitate was filtered to the heating stage and heated at 600 °C in furnace for 2 hours to form CdS powder.

### 2.3. Oxygen Doping

The green synthesized CdS powder was heated at 200°C with a constant oxygen flow rate of 0.25 L/min. This doping process was carried out in a tubular furnace system, and CdS-O was formed with a time variation of 30, 60, and 120 minutes (CdS-O 30, CdS-O 60, and CdS-O 120).

### 2.4. Characterization

The difference in functional groups of bare CdS and oxygen-doped CdS (CdS-O) was observed by FTIR spectrophotometer analysis. In addition, the crystal size and crystallinity peak also was measured by X-ray diffraction (XRD) analysis using a Bruker D2 Phaser XRD (Cu-K $\alpha$ , Ni filter). Meanwhile, optical properties and band gap energy

was measured with a UV-DRS spectrophotometer instrument. Meanwhile, the films' surface morphology and elemental composition were determined using a Phenom Desktop ProXL Analytical 20 kV scanning electron microscope (SEM) equipped with a Swift ED3000 energy dispersive X-ray spectrometer (EDX). A UV-Vis spectrophotometer also was used to calibrate and measure the photodegradation performance.

### 2.5. Application of ciprofloxacin photodegradation

The ciprofloxacin samples used first were calibrated to ensure the accuracy of the concentration and maximum wavelength values. Calibration was done by preparing solutions of 10, 15, 20, 25 and 30 ppm CIP. Each concentration was observed for absorbance with a UV-Vis spectrophotometer. In addition, photo degradation applications then were carried out with variations in degradation time of 15, 30, 45, 60, 75, 105, and 120 minutes to observe the kinetics and reaction order.

## 3. Results and Discussion

### 3.1. FTIR Analysis

FTIR was used to evaluate the functional groups in a material/compound on the synthesized cadmium sulfide (CdS) and oxygen-doped cadmium sulfide (CdS-O) samples, as Figure 1. There is no significant difference in spectra between bare CdS and oxygen-doped CdS. The absorption bands in the 400-700  $\text{cm}^{-1}$  wavenumber range caused by the Cd-S stretching vibrational mode. Peaks around 3056  $\text{cm}^{-1}$  and 3223.85  $\text{cm}^{-1}$  are O-H stretch vibrations of  $\text{H}_2\text{O}$  molecules attached to the sample surface [22]. The peaks between 1540  $\text{cm}^{-1}$  and 1551  $\text{cm}^{-1}$  are carbon double bonds with oxygen (C=O) associated with amide groups such as polyphenols, proteins, and amino acids [23].

Other readable peaks indicate C-C bonds shown at 990.15  $\text{cm}^{-1}$  and 991.13  $\text{cm}^{-1}$ . The peaks between 1009  $\text{cm}^{-1}$  and 1163  $\text{cm}^{-1}$  assigned to S-O stretching vibrations of sulfate groups, and these peaks were due to the presence of trace contaminants resulting from the reaction between the precursor and the solvent [24]. This indicates that doping does not involve changing the chemical bonds and lattice of CdS; oxygen acts as an impurity, forming covalent bonds with atoms around the doping site. However, it can lead to the formation of complexes involving multiple covalent bonds between oxygen and the surrounding atoms, altering the electronic and structural properties of the material, such as changes in band gap and composition of S and O elements [25-26].

### 3.2. Crystal Structure

The XRD patterns of the samples can provide information about the crystallinity phase and the actual compounds of the samples obtained from the synthesis and doping processes. The XRD patterns of CdS and CdS-O 120 are shown in Figure 2, plotted against the CdS (Hexagonal) database no. 1011054 [27]. Based on the XRD spectra obtained, the XRD pattern shows that the diffraction patterns between CdS and CdS-O are similar. The results of the analysis both show the similarity of peaks with the CdS database CdS (Hexagonal) no. 1011054 with peaks appearing at angles 24.95° (1 0 0); 26.48° (0 0 2); 28.28° (1 0 1); 43.66° (1 0 2); 45.79° (1 1 1); 47.8° (1 1 0); 51.71° (1 1 2) and 60.68° (0 1 4). After matching with the database, it concluded that

the preparation of cadmium sulfide by green synthesis and doping method successfully formed CdS nanoparticles.

The match of XRD analysis data with data in the Match application explains that the sample obtained has a hexagonal crystal shape; based on COD (Crystallography Open Database) diffraction data, the sample used has lattice parameters  $a = 4.15000 \text{ \AA}$ ,  $c = 6.73700 \text{ \AA}$  [27]. The crystal size calculated based on the Full Width at Half Maximum (FWHM) values at various peaks with the Debye-Scherrer equation (1) [28]:

$$G = \frac{k \lambda}{D \cos \theta} \quad (1)$$

Where  $G$  is the crystal size,  $k = 0.9$  is the formation factor,  $\lambda$  is the wavelength of the  $\text{CuK}\alpha$  line,  $D$  is the FWHM in radians, and  $\theta$  is the Bragg angle. The calculation results in Table 1 reveal the crystal size calculation. The average crystal size of CdS and CdS-O are 28.16 nm and 19.46 nm, respectively. These sizes include nanometer-sized crystals because the size of nanoparticle crystals ranges from 0 to 100 nm [6-24].

### 3.3. Energy Gap Band

UV-DRS analysis used to determine the energy gap of the analyzed sample and relate it to the photo degradation effect during the photo catalytic process of ciprofloxacin degradation to obtain the energy gap ( $E_g$ ) graph. The known semiconductor band gap in Figure 3 explains that the energy gap possessed by CdS-O is smaller when compared to CdS without doping, with the  $E_g$  value of CdS being 2.37 eV while  $E_g$  CdS-O 120 is 2.35 eV. The smaller the energy gap of a catalyst, the greater the effectiveness of the photo catalyst because the absorption of photons ( $h\nu$ ) requires smaller energy. In addition to reducing the energy gap, oxygen doping also helps CdS to trap electrons to reduce the possibility of electron-hole recombination [17]. Oxygen doping can affect the probability of electronic transition between the valence band and the conduction band. This can affect optical and photo catalytic absorbance.

In an isoelectronic impurity in a semiconductor whose bonding is predominantly covalent, the electrons contributing to the covalent bond will tend towards the electronegative atom, and the resulting polarization will remain on the impurity. When the electron density between the impurity and the nearest neighboring atom is insufficient to produce polarization or charged atoms, electrons will be supplied from the host atom to the electronegative impurity; that is, charge transfer occurs. This phenomenon can occur in ionic semiconductors such as CdS [26-29]. Table 2 shows oxygen doping on CdS can decrease band gap energy ( $E_g$ ). As the band gap reduced, it narrows, producing many photo-induced charge carriers in photocatalysis [17-26]. Therefore, CdS-O obtained with better light absorption and a narrower band gap expected to present better photocatalysis activity.

### 3.4. Morphology and Elemental Distribution

SEM was used to investigate the structure of the CdS samples. SEM images were recorded and shown in Figure 4. As shown, the morphology of CdS and CdS-O have different shapes. CdS has a surface morphology that tends to look more like a ball, but the morphology of CdS-O looks like a coral. It is exactly as stated in the literature [30], that quercetin helps in agglomeration stability. Figure 4. Shows that the surface shape of CdS without doping stably agglomerated, so its

shape is spherical and regular. CdS-O is coral-like, according to the literature [31]. The heating effect causes a transformation of shape and structure from spherical CdS to an irregular structure with a larger surface area. Table 3. Shows a little carbon content in both samples due to the use of organics in the synthesis process, which still attached to the sample's surface. Then, the appearance of oxygen in CdS, even without the doping process, is because heating does not isolate oxygen in the furnace, so it is possible that heating in the furnace still has oxygen affecting the CdS sample. The increase in oxygen also confirms the occurrence of oxygen doping on the surface. In addition, the decrease in Cd and S predicted as the effect of defects that may occur in either S-vacancy or other bonds, as the literature shows [26-29].

### 3.5. Application of ciprofloxacin photodegradation

The maximum wavelength of ciprofloxacin was determined, and a graph showing the comparison between the absorbance of ciprofloxacin with different concentration variations and the maximum wavelength is obtained, as shown in Figure 5. The graph has two peaks, including 278 nm and 319 nm [32], read at each peak (Fig. 5a). The data obtained were processed into a curve with the concentration relationship as the x-axis and absorbance as the y-axis to obtain the line equation  $y = mx + c$ . Figure 5b shows the linear relationship of concentration to absorbance following the Lambert-Beer law. The 319 nm wavelength used because the r-value (correlation coefficient) is closer to one, showing a stronger linear relationship than 278 nm. The degradation test was conducted to determine the ability level of CdS and CdS-O (30, 60, 120 min) catalysts in degrading ciprofloxacin solution. The degradation test carried out by mixing CdS powder in ciprofloxacin solution and stirring in the dark with a measured time to achieve equilibrium absorption - desorption of ciprofloxacin on the catalyst surface [33].

After reaching equilibrium, the irradiation and stirring process were continued with a measured time. The results of the photo catalytic degradation were tested using UV-Vis spectrophotometer, and the results shown in Figure 6. The degradation diagram above shows the percentage level of photo catalytic degradation of ciprofloxacin by CdS and CdS-O. The data shows that as time increases, the percentage of degradation produced increases and occurs in each sample. The highest percentage of degradation are obtained from CdS, CdS-O 30, CdS-O 60, and CdS-O 120 were 41.5%, 50.5%, 53.1%, and 58.5%, respectively. This proves that adding oxygen doping can increase the effectiveness in the degradation of ciprofloxacin solution. The degradation kinetics obtained is shown in Figure 7. In determining the degradation rate of ciprofloxacin with CdS and CdS-O (30; 60; 120) catalysts, the first order pseudo degradation kinetics equation (2) [34] was used:

$$kt = \ln \frac{C_0}{C} \quad (2)$$

$C_0$  is the initial concentration of ciprofloxacin,  $C$  is the concentration of ciprofloxacin at a certain time variation ( $t$ ), and  $k$  indicates the constant degradation rate. The observed degradation rate constant was determined by plotting  $\ln(C/C_0)$  against the time ( $t$ ) of the observed ciprofloxacin concentration. The graph explains that each sample increases its reaction rate; the longer the irradiation time, the greater the degradation rate.

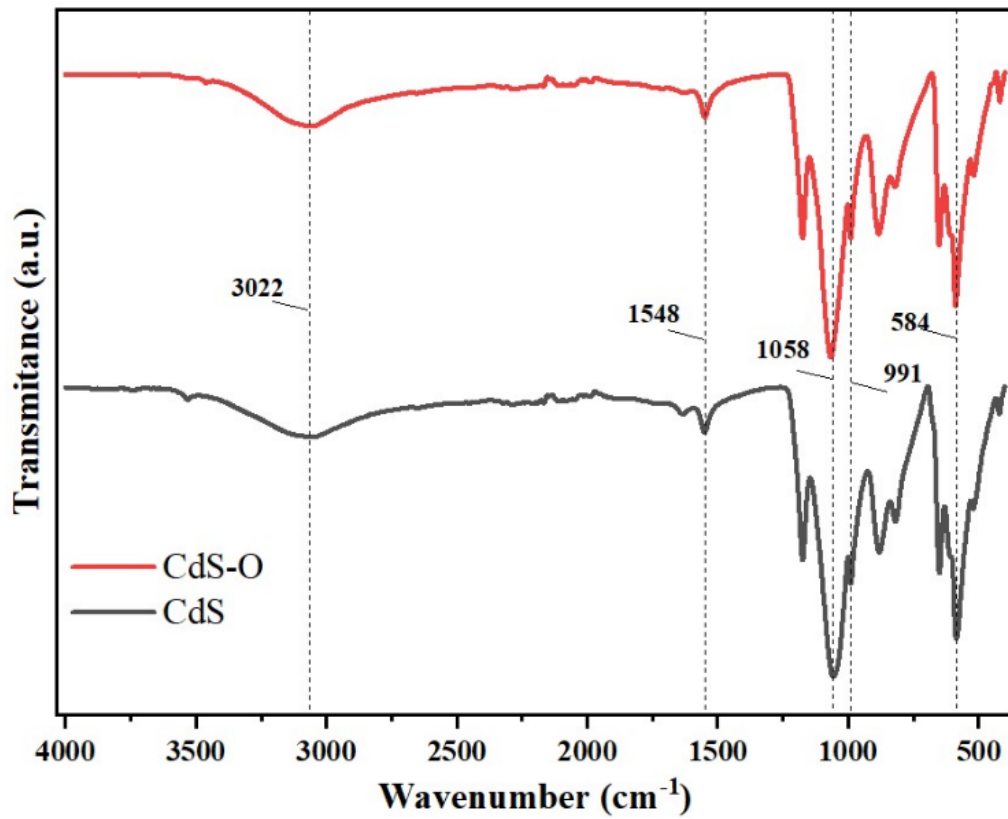


Figure 1. FTIR spectra of CdS and CdS-O.

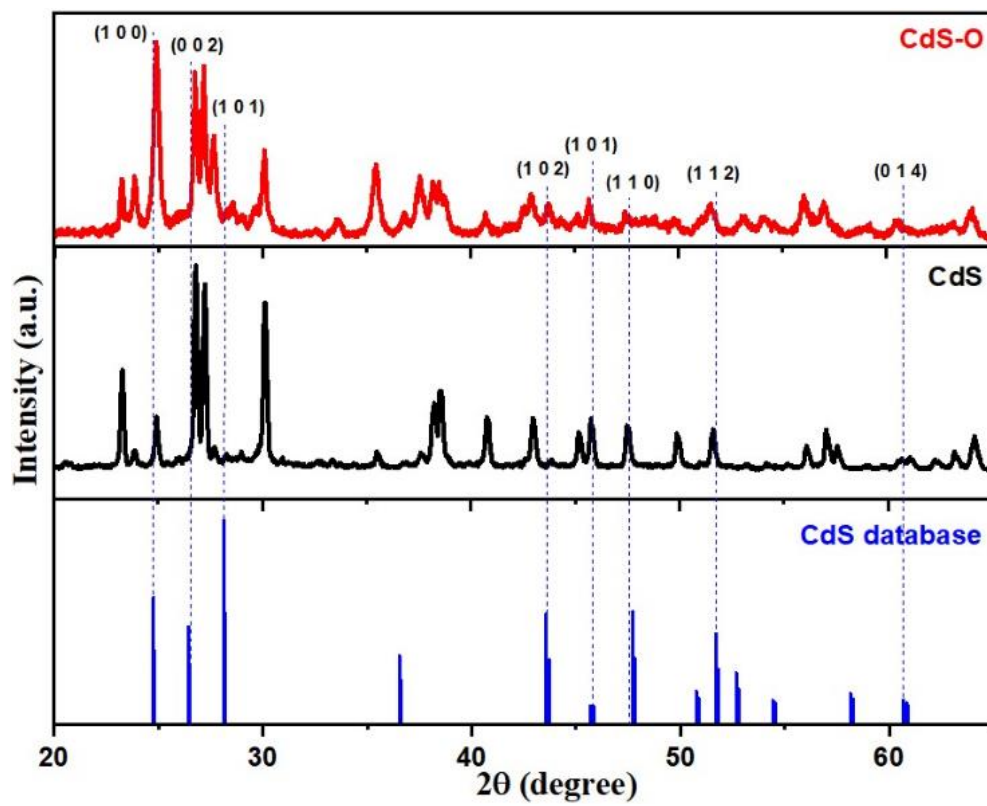


Figure 2. XRD diffractogram of CdS, CdS-O, and CdS database.

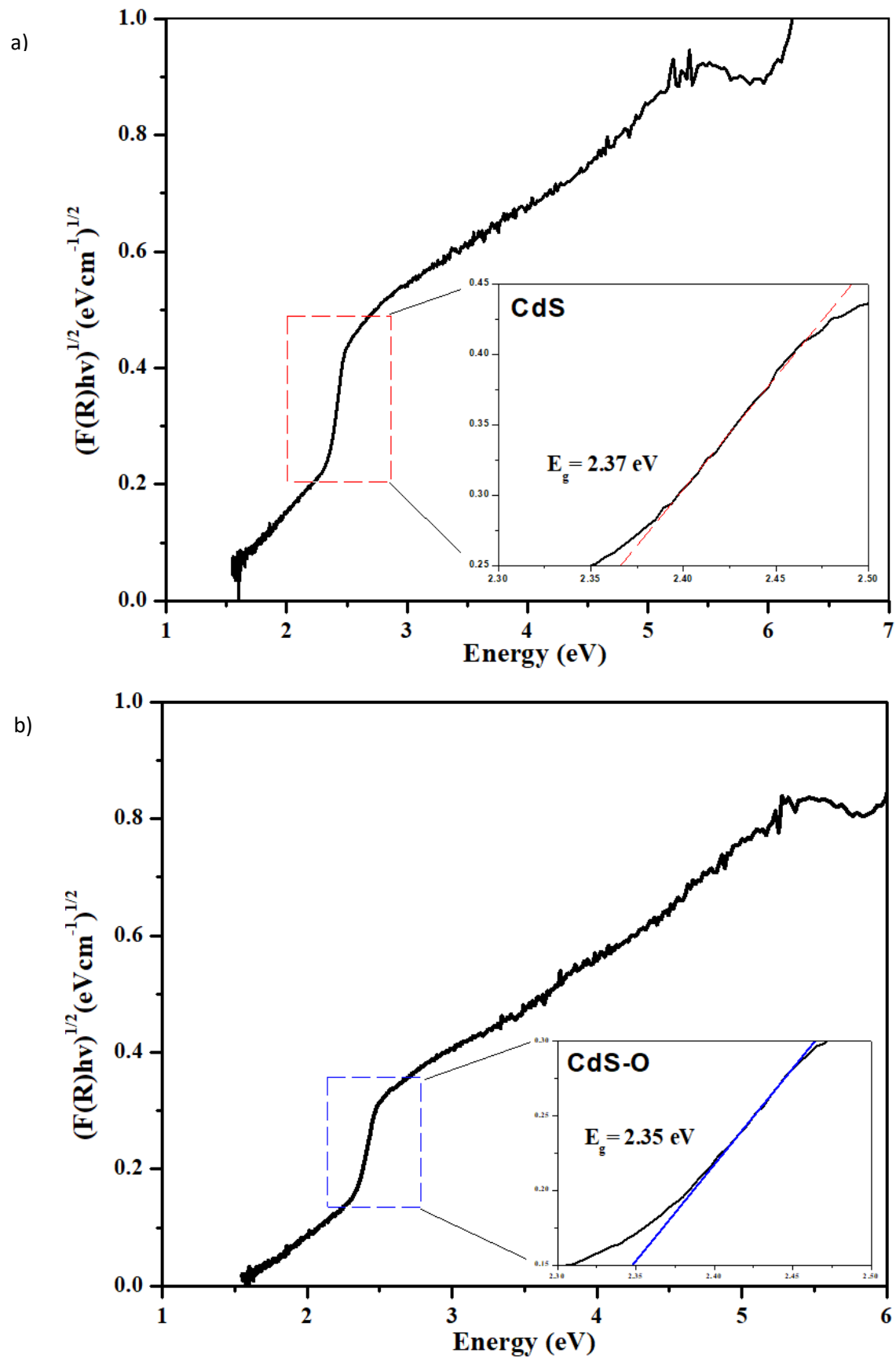
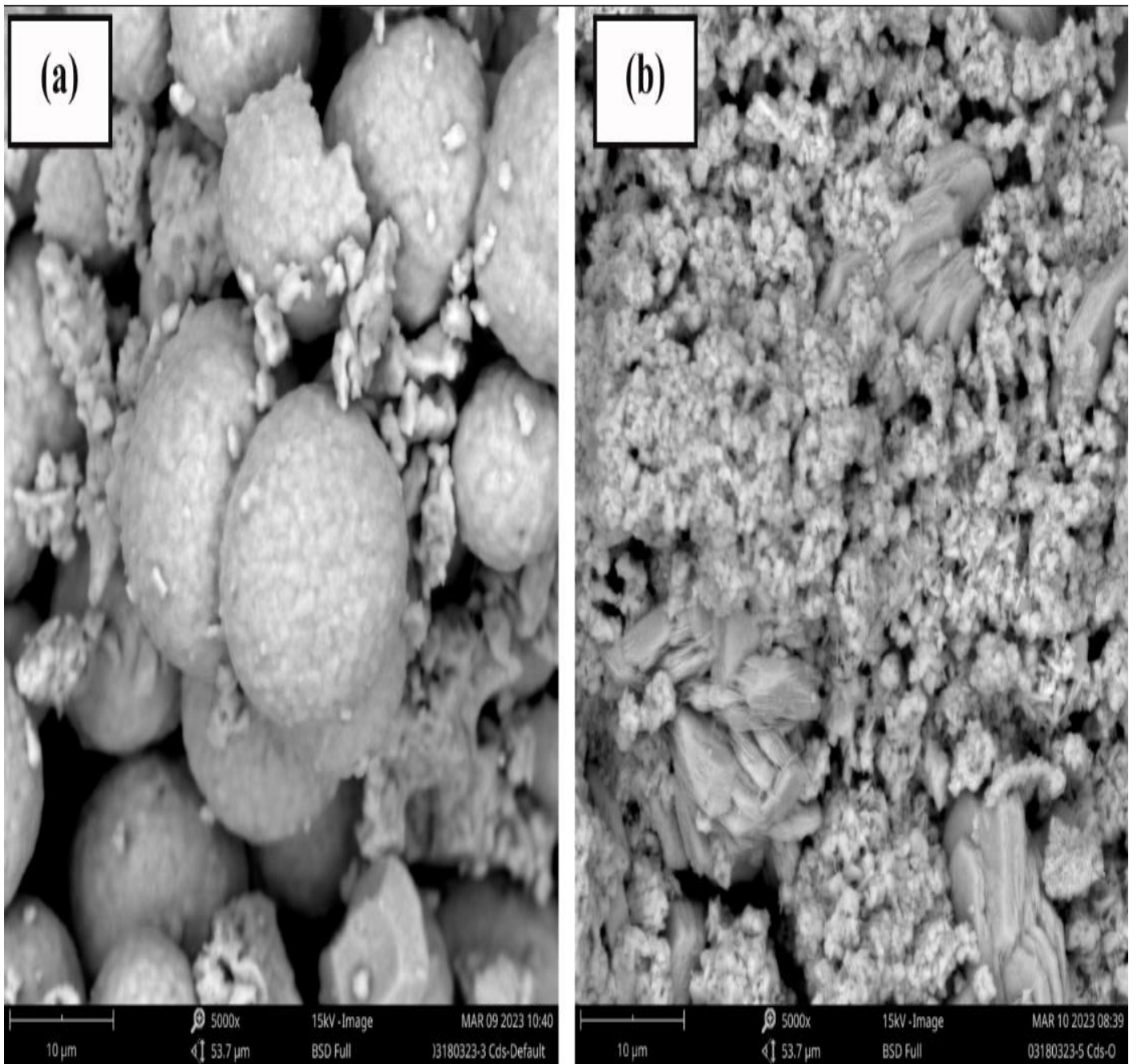


Figure 3. Energy band graph of CdS (a) and CdS-O (b).





**Figure 4.** Surface morphology of CdS (a) and CdS-O (b) at 5000x magnification.

**Table 1:** Crystal size of CdS and CdS-O particles

Sample	2 $\theta$ ( $^{\circ}$ )	FWHM( $^{\circ}$ )	D (nm)
<b>CdS</b>	24.93	0.19098	42.60
	26.82	0.73336	11.14
	28.28	0.21101	38.83
	43.86	39.06734	0.22
	45.75	0.21759	39.63
	47.48	0.22156	39.17
	51.60	0.22768	38.76
	60.68	0.61551	14.96
	Average		28.16
<b>CdS-O</b>	24.85	0.32636	24.93
	26.74	1.11371	7.33
	28.57	0.26939	30.43
	43.78	0.55836	15.33
	45.67	62.6659	0.14
	47.42	62.8773	0.14
	51.56	0.34406	25.64
	60.58	0.17769	51.78
	Average		19.46

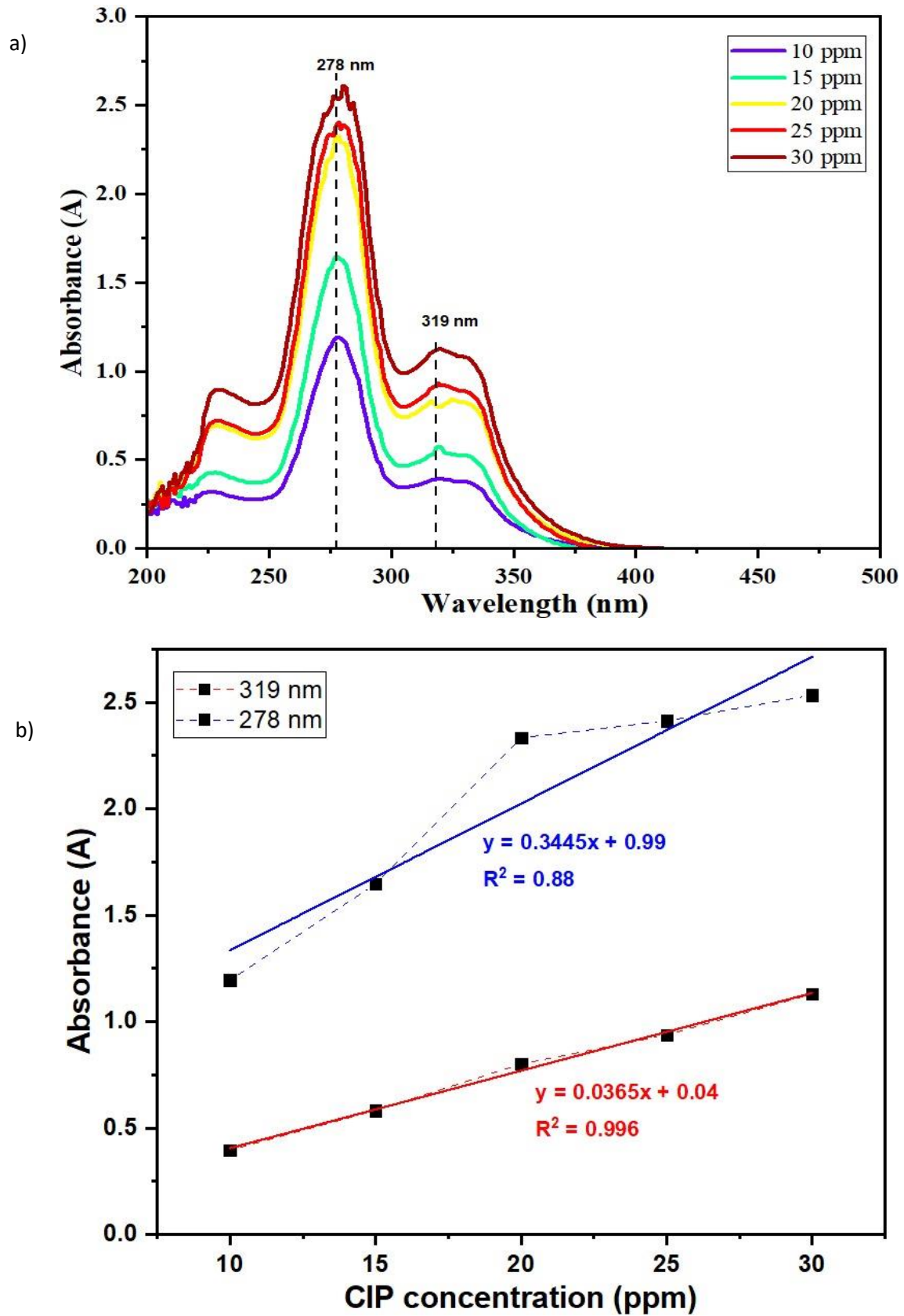


Figure 5. Absorbance spectra of CIP at varying concentrations (a) and calibration curves of maximum wavelength peak (b).



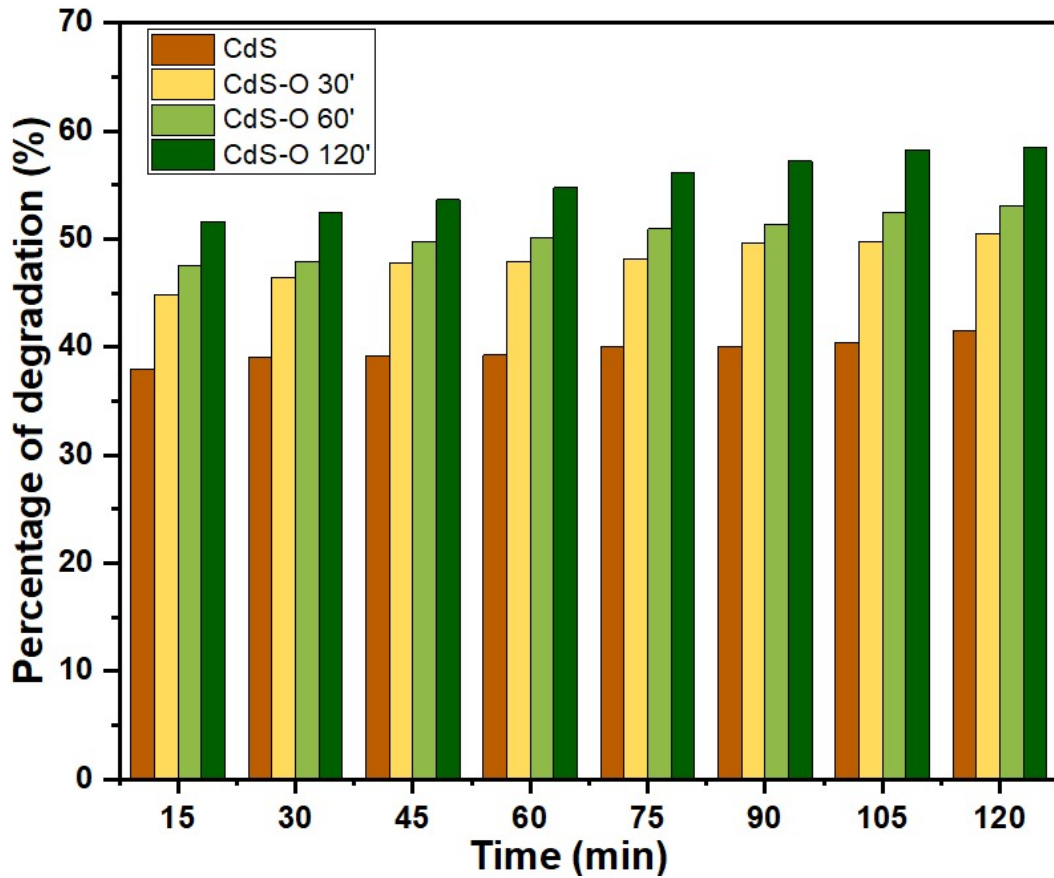


Figure 6. Percentage of CIP degradation by CdS and CdS-O with time variation.

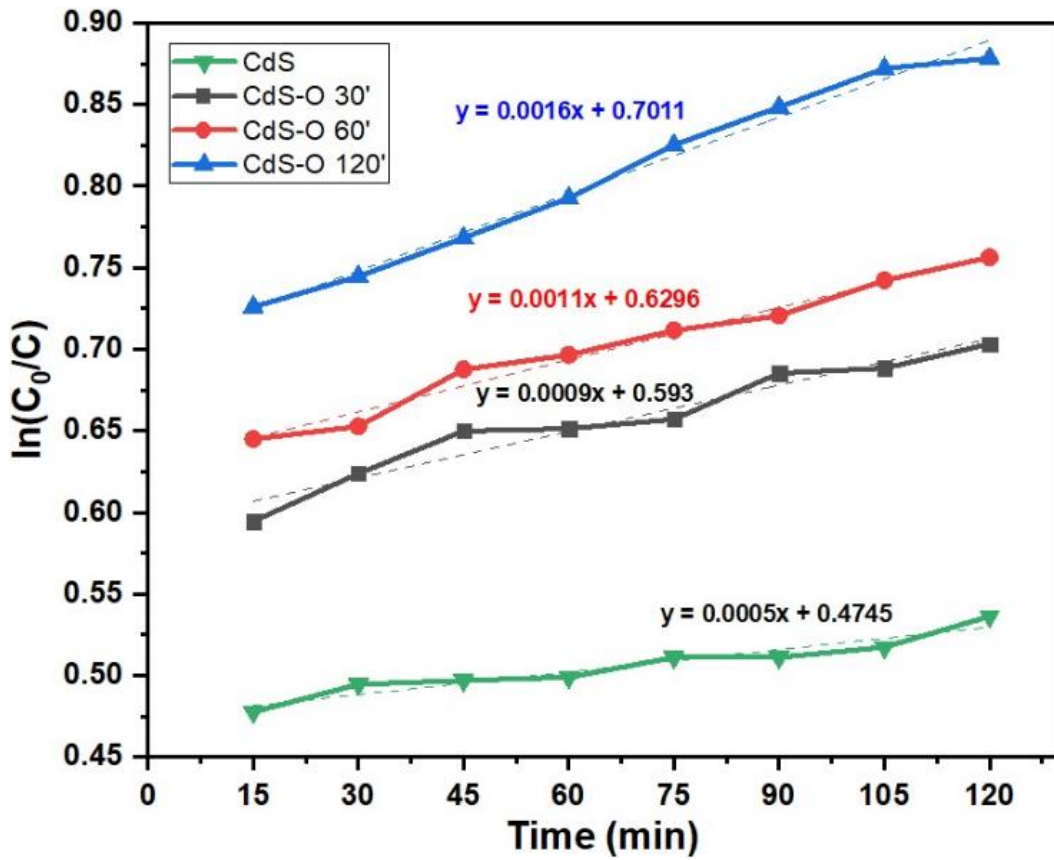


Figure 6. Percentage of CIP degradation by CdS and CdS-O with time variation.

**Table 2:** Values of band gap energy ( $E_g$ ) and maximum wavelength of absorbance of CdS and CdS-O

Sample	Wavelength (nm)	Band gap energy (eV)
CdS	523.21 nm	2.37 eV
CdS-O	527.66 nm	2.35 eV

**Table 1:** Elemental composition on the surface of CdS and CdS-O samples from EDX analysis.

Sample	Element	Atom concentration (%)	Weight concentration (%)
CdS	Cd	27.34	69.23
	O	49.22	17.74
	S	14.81	10.7
	C	8.63	2.34
CdS-O	Cd	19.54	60.28
	O	59.42	26.09
	S	12.18	10.72
	C	8.86	2.92

The value of the relationship coefficients ( $r$ ) obtained explain that the relationship of the degradation rate at the irradiation time of the CdS, CdS-O 30, CdS-O 60, and CdS-O 120 samples are 0.961, 0.971, 0.989, and 0.994, respectively. The obtained reaction kinetics results prove that the percentage of ciprofloxacin degradation is directly proportional to the obtained degradation rate.

#### 4. Conclusions

Synthesis of modified cadmium sulfide (CdS) via green synthesis and doped with oxygen (CdS-O), followed by testing its effectiveness in the photo catalytic degradation of ciprofloxacin has been successfully carried out. Green synthesis using tea powder resulted in smaller particles and oxygen doping, helping to reduce the band gap and increasing its effectiveness in the photo degradation of ciprofloxacin. Characterization of synthesized CdS and CdS-O indicates that doping does not involve changing the chemical bonds and lattice; oxygen acts as an impurity, forming covalent bonds with atoms around the doping site. FTIR shows functional groups typical of CdS in the fingerprint area. XRD shows the similarity of peaks with the CdS database, with the average crystal size of nanoparticles decreasing with doping; CdS and CdS-O are 28.16 nm and 19.46 nm, respectively. SEM analysis shows that CdS particles have a smooth and spherical surface, while CdS-O particles show a coral-like structure. Oxygen doping reduces the band gap of CdS from 2.37 eV to 2.35 eV. Ciprofloxacin (CIP) degradation results show that CdS-O achieves a better degradation effect than CdS, with the degradation percentage reaching 58.5%. This highlights the development potential of green synthesis methods and enhanced photocatalytic properties for wastewater treatment.

#### References

- [1] M. Zhang, Y. Zhang, Y. Zhu, J. Wang, L. Qiao, Y. Zhao, Y. Tao, Y. Xiao, L. Tang. (2023). Insights into adsorption and high photocatalytic oxidation of ciprofloxacin under visible light by intra-molecular Donor-Acceptor like pn isotype heterojunction: Performance and mechanism. *Chemical Engineering Journal*. 464: 142533.
- [2] D. Gu, S. Zhang, T. Jiang, H. Jiang, X. Wang, B. Wang. (2020). Positive P/g-C<sub>3</sub>N<sub>4</sub> thermo-coupled photocatalytic oxidation of refractory organics in wastewater for total utilization of solar Vis-IR region. *Materials Chemistry and Physics*. 253: 123307.
- [3] D. Van Thuan, T.B. Nguyen, T.H. Pham, J. Kim, T.T.H. Chu, M.V. Nguyen, K.D. Nguyen, W.A. Al-Onazi, M.S. Elshikh. (2022). Photodegradation of ciprofloxacin antibiotic in water by using ZnO-doped g-C<sub>3</sub>N<sub>4</sub> photocatalyst. *Chemosphere*. 308: 136408.
- [4] X. Hu, X. Hu, Q. Peng, L. Zhou, X. Tan, L. Jiang, C. Tang, H. Wang, S. Liu, Y. Wang. (2020). Mechanisms underlying the photocatalytic degradation pathway of ciprofloxacin with heterogeneous TiO<sub>2</sub>. *Chemical Engineering Journal*. 380: 122366.
- [5] S. Liang, G. Sui, D. Guo, Z. Luo, R. Xu, H. Yao, J. Li, C. Wang. (2023). g-C<sub>3</sub>N<sub>4</sub>-wrapped nickel doped zinc oxide/carbon core-double shell microspheres for high-performance photocatalytic hydrogen production. *Journal of Colloid and Interface Science*. 635: 83-93.
- [6] R.A. Wijaya, A. Suseno, R.A. Lusiana, W. Septina, T. Harada. (2023). Synthesis of CuInS<sub>2</sub> thin film photocathode with variation of sulfurization sources and Pt-In<sub>2</sub>S<sub>3</sub> modification for photoelectrochemical

- water splitting. *Journal of Electroanalytical Chemistry*. 945: 117683.
- [7] B.M. Namoos, A.R. Mohamed, K.A. Ali. (2023). Methods and strategies for producing porous photocatalysts. *Journal of Solid State Chemistry*. 320: 123834.
- [8] A. Regmi, Y. Basnet, S. Bhattarai, S.K. Gautam. (2023). Cadmium sulfide nanoparticles: synthesis, characterization, and antimicrobial study. *Journal of Nanomaterials*. 2023(1): 8187000.
- [9] A.D. Terna, E.E. Elemike, J.I. Mbonu, O.E. Osafire, R.O. Ezeani. (2021). The future of semiconductors nanoparticles: Synthesis, properties and applications. *Materials Science and Engineering: B*. 272: 115363.
- [10] A. Ghasempour, H. Dehghan, M. Ataei, B. Chen, Z. Zhao, M. Sedighi, X. Guo, M.-A. Shahbazi. (2023). Cadmium sulfide nanoparticles: preparation, characterization, and biomedical applications. *Molecules*. 28(9): 3857.
- [11] A. Nivetha, S. Mangala Devi, I. Prabha. (2019). Fascinating physic-chemical properties and resourceful applications of selected cadmium nanomaterials. *Journal of Inorganic and Organometallic Polymers and Materials*. 29: 1423-1438.
- [12] K. Shivaji, S. Mani, P. Ponnuragan, C.S. De Castro, M. Lloyd Davies, M.G. Balasubramanian, S. Pitchaimuthu. (2018). Green-synthesis-derived CdS quantum dots using tea leaf extract: antimicrobial, bioimaging, and therapeutic applications in lung cancer cells. *ACS Applied Nano Materials*. 1(4): 1683-1693.
- [13] S. Tudu, M. Zubko, J. Kusz, A. Bhattacharjee. (2021). CdS nanoparticles (< 5 nm): green synthesized using *Termitomyces heimii* mushroom-structural, optical and morphological studies. *Applied Physics A*. 127: 1-9.
- [14] S. Munyai, Z. Tetana, M. Mathipa, B. Ntsendwana, N. Hintsho-Mbita. (2021). Green synthesis of Cadmium Sulphide nanoparticles for the photodegradation of Malachite green dye, Sulfisoxazole and removal of bacteria. *Optik*. 247: 167851.
- [15] E.M. Bakhsh, M.I. Khan. (2022). Clove oil-mediated green synthesis of silver-doped cadmium sulfide and their photocatalytic degradation activity. *Inorganic Chemistry Communications*. 138: 109256.
- [16] Z.K. Heiba, M.B. Mohamed, A. Badawi. (2021). Structure, optical and electronic characteristics of iron-doped cadmium sulfide under nonambient atmosphere. *Applied Physics A*. 127: 1-11.
- [17] R.K. Chava, N. Son, M. Kang. (2021). Controllable oxygen doping and sulfur vacancies in one dimensional CdS nanorods for boosted hydrogen evolution reaction. *Journal of Alloys and Compounds*. 873: 159797.
- [18] J. Hou, S. Cao, Y. Sun, Y. Wu, F. Liang, Z. Lin, L. Sun. (2018). Atomically thin mesoporous  $\text{In}_2\text{O}_3-x/\text{In}_2\text{S}_3$  lateral heterostructures enabling robust broadband-light photo-electrochemical water splitting. *Advanced Energy Materials*. 8(9): 1701114.
- [19] A. Liu, M. Gao, Y. Ma, X. Ren, L. Gao, Y. Li, T. Ma. (2021). Theoretical study of the influence of doped oxygen group elements on the properties of organic semiconductors. *Nanoscale Advances*. 3(11): 3100-3106.
- [20] L. Meng, D. Rao, W. Tian, F. Cao, X. Yan, L. Li. (2018). Simultaneous manipulation of O-doping and metal vacancy in atomically thin  $\text{Zn}_{10}\text{In}_{16}\text{S}_{34}$  nanosheet arrays toward improved photoelectrochemical performance. *Angewandte Chemie International Edition*. 57(51): 16882-16887.
- [21] M.S. Alqahtani, N. Hadia, S. Mohamed. (2019). Tuning the optical, electrical resistivity and structural properties of DC magnetron sputtered aluminum zinc oxide films by changing the oxygen flow rate. *Applied Physics A*. 125(11): 776.
- [22] R.K. Sonker, B. Yadav, V. Gupta, M. Tomar. (2020). Synthesis of CdS nanoparticle by sol-gel method as low temperature  $\text{NO}_2$  sensor. *Materials Chemistry and Physics*. 239: 121975.
- [23] C.K. Sheng, Y.M. Alrababah. (2023). pH-induced wurtzite-zinc blende heterogeneous phase formation, optical properties tuning and thermal stability improvement of green synthesized CdS nanoparticles. *Heliyon*. 9(5).
- [24] B.S. Goud, Y. Suresh, S. Annapurna, A. Singh, G. Bhikshamaiah. (2016). Green synthesis and characterization of cadmium sulphide nanoparticles. *Materials Today: Proceedings*. 3(10): 4003-4008.
- [25] Q. Wu, X. Lin, H. Mahabaduge, X. Liu, Y. Zhang. (2022). Effect of oxygen on the properties of CdSe thin films prepared by RF-sputtering. *Chemical Physics Letters*. 799: 139633.
- [26] M. Islam, H. Misran, M. Akhtaruzzaman, N. Amin. (2020). Influence of oxygen on structural and optoelectronic properties of CdS thin film deposited by magnetron sputtering technique. *Chinese Journal of Physics*. 67: 170-179.
- [27] D. Fuhrmann, N.H. Bollfraß, M. Icker, H. Krautscheid. (2023). Synthesis, X-ray Diffraction, NMR and Thermolysis Studies of Cadmium Tin Sulfido Complexes. *Crystals*. 13(5): 721.
- [28] G. Gunawan, S.G.L. Megawati, N.B.A. Prasetya, R.A. Wijaya. (2022). Synthesis, Characterization of  $\text{Ag}_2\text{S}$  from  $\text{AgCl}$  Waste of Argentometry Titration with Heating Temperature Variations and Its Application as a Temperature Sensor Based on Negative Temperature Coefficient (NTC). *Jurnal Kimia Sains dan Aplikasi*. 25(8): 292-299.
- [29] K. Akimoto, H. Okuyama, M. Ikeda, Y. Mori. (1992). Oxygen doping in CdTe, CdS and ZnS. *Journal of crystal growth*. 117(1-4): 420-423.
- [30] S. Jain, M.S. Mehata. (2017). Medicinal plant leaf extract and pure flavonoid mediated green synthesis of silver nanoparticles and their enhanced antibacterial property. *Scientific reports*. 7(1): 15867.
- [31] G.V.J. Dantas, N.P. de Moraes, R. Bacani, L.A. Rodrigues. (2022). Facile synthesis of cadmium sulfide and the effect of thermal annealing in  $\text{N}_2$ -rich

- atmosphere on its structural, morphological, chemical, and optical properties. *Materials Chemistry and Physics*. 277: 125492.
- [32] G. Gunawan, N.B.A. Prasetya, R.A. Wijaya. (2023). Degradation of Ciprofloxacin (CIP) Antibiotic Waste using The Advanced Oxidation Process (AOP) Method with Ferrate (VI) from Extreme Base Electrosynthesis. *Trends in Sciences*. 20(7): 6639-6639.
- [33] Y. Zhang, H. Pan, F. Zhang. (2019). Solvothermal synthesis of CDs/Bi<sub>4</sub>O<sub>5</sub>Br<sub>2</sub> nanocomposites with improved visible-light photocatalytic ciprofloxacin (CIP) decontamination. *Materials Letters*. 251: 114-117.
- [34] M.R. Usman, A. Prasasti, S. Islamiah, A.N. Firdaus, A.W. Marita, S. Fajriyah, A.R. Noviyanti, D.R. Eddy. (2021). Degradation of ciprofloxacin by titanium dioxide (TiO<sub>2</sub>) nanoparticles: Optimization of conditions, toxicity, and degradation pathway. *Bulletin of Chemical Reaction Engineering & Catalysis*. 16(4): 752-762.